Finite Element Modelling of Flat Slabs Strengthened with Shear Bolts with Small and Large Anchorages

Thamer Hussein Amer[1*] , Hussein Riyadh Taresh[1] , Zainab Abdulameer Sabur[1] , Mohd Yazmil Md Yatim[2]

[1] College of Engineering, University of Sumer, Rifai 64005, Iraq
[2] Department of Civil Engineering, Universiti Kebangsaan Malaysia, UKM Bangi 43600, Malaysia

Corresponding Author Email: Hussein.Riyadh@uos.edu.iq

ABSTRACT

This paper numerically studies the punching shear response of flat slabs strengthened by shear bolts with two kinds of end anchorages. The anchorages of shear bolts involve small and large anchorages on slab surfaces. The study intends to provide distinctive numerical modelling techniques for modelling and analysing shear-reinforced flat slabs using shear bolts. Moreover, it intends to investigate the proper arrangements of shear bolts for resisting punching shear. The numerical analyses were conducted using the concrete damaged plasticity (CDP) in ABAQUS software. For validation and assessments, eight interior tested junctions from a previous study were selected. One of them was without strengthening, while the others were strengthened against punching shear using shear bolts. The study presented and compared maximum failure loads, the behaviour of both flexural and shear reinforcements, and crack patterns with the test outcomes. The numerical results revealed that employing beams and solid elements to model shear bolts and their anchorages, respectively, was the optimal choice. Additionally, the numerical results showed that adopting a radial arrangement of shear bolts with large anchorages was optimal for punching shear reinforcement. The obtained numerical data were compared with the predicted failure loads from the design codes.

1. INTRODUCTION

Slab-column junctions in flat slabs without shear reinforcement are highly susceptible to punching shear failure, a kind of brittle failure that occurs without prior warning signs. In certain cases, the punching shear strength of these junctions may be insufficient due to many circumstances, including changes in building usage, design or construction mistakes, reinforcing corrosion, and concrete degradation. Typically, this failure occurs when the externally applied shear stresses surpass the tensile strength of the concrete. Therefore, it is essential to recommend appropriate shear reinforcement for this purpose. Numerous researchers over years have proposed and investigated various punching shear reinforcements for new and existing flat slabs.

Numerous researchers performed experiments in testing and evaluating different kinds of shear reinforcements for the new flat slabs, such as stirrups, bent-up bars, shear studs, truss-shear reinforcement, and shear heads. Shear reinforcement can be added around the column where bending and shear stresses are at their highest levels to enhance the shear resistance and ductility of the slab. Shear reinforcement is positioned to intercept the inclined cracks within the slab depth. Bent-up bars were utilised by references [1, 2]. Closed stirrups were examined by references [3-7]. Shear heads were examined by references [8-10]. Shear studs were utilised by references [11,

12]. Pre-assembled truss bars were deeply investigated by reference [13].

There are three distinct approaches to strengthening existing flat slabs: 1) By expanding the supporting territory, hence increasing the critical section around the column [14-16]. This would improve the flexural capacity of the slab. Nonetheless, the slab-column connections demonstrate comparatively more brittle behaviour. 2) Implementing post-installed shear reinforcements [17-21], including shear bolts and concrete screws. This method considerably enhances the ductility of slab-column connections. Typically, the slab will fail before the complete activation and shear bolts. 3) Enhancing the flexural tension reinforcement by adding an additional layer of concrete or affixing an external reinforcement composed of carbon fibre-reinforced polymers (CFRP) or steel [22-24]. This approach increases the effective depth of the slab, hence increasing its flexural strength; nevertheless, it concurrently leads to increased brittleness in the slab-column connections.

The shear bolt strengthening system with small end anchorages on slab surfaces, an innovative kind of punching shear reinforcement invented by reference [25], was then deeply investigated by reference [19] in the interior slab-column junctions. The references [17-20] conducted several investigations into this kind of strengthening strategy and proved its effectiveness in resisting punching shear in flat slabs. The existing literature lacks a thorough numerical

modelling and analysing of shear bolts with two anchorage strategies: small and large anchorages on slab surfaces. However, limited numerical studies conducted by Genikomsou and Polak [26, 27] modelled and analysed reinforced flat slabs with shear bolts incorporating small end anchorages on slab surfaces. They discovered that the best way to model shear bolts is with the beam element type (B32). To avoid concrete failure at anchorages, they also simulated the small end anchorages of shear bolts using assembled beam elements with a size larger than the actual anchorages, provided that they overlap with each other (see Figure 1). However, the current literature still lacks numerical studies related to modelling large anchorages of shear bolts. This approach relies on assumptions that complicate the modelling process, while other simple and reliable techniques have not yet been investigated. Investigating these simpler techniques may provide valuable insights and lead to more precise results. Furthermore, there are a few recent studies concerning the utilisation of diverse configurations of shear bolts, particularly in conjunction with large-end anchorages. All previous studies concentrated on shear bolts with small end anchorages.
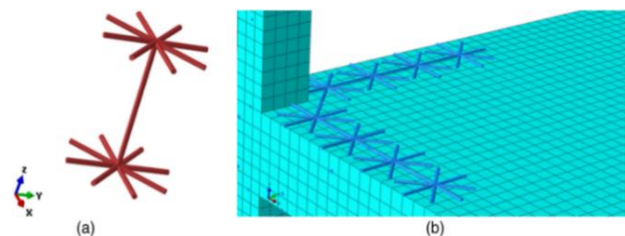

Figure 1. Assembled truss/beam for shear bolt modelling [26]

In this study, the concrete damaged plasticity (CDP) model in ABAQUS is used to numerically calibrate eight interior slab-column junctions shear-reinforced by shear bolts with large and small anchorages to slab surfaces originally tested by reference [28]. The study proposes numerical modelling approaches for representing the end anchorages of shear bolts and assesses the efficacy of the strengthening method for ultimate capacity, failure mode, ductility, stiffness, and energy absorption. Besides, it investigates the various arrangements of shear reinforcements around the supporting region and their impact on the structural integrity. The numerical results are ultimately compared to the applicable design code standards to assess their consistency and identify potential areas for improvement.

2. TEST SLABS

2.1 Description of tested slabs

Eight large-scale slabs representing interior slab-column junctions were prepared and monotonically tested to failure by reference [28]. Seven specimens were strengthened using post-installed vertical shear bolts, while the last one was examined without any shear enhancement to serve as a reference slab. The slabs were square in shape, with side dimensions of 1800 mm and a depth of 120 mm. They represent the region surrounding a column of an interior slab panel up to zero moment lines (contraflexure). The upper flexural reinforcement (tension side) consisted of reinforcing bars of 10 mm spaced at 200 mm with concrete cover 20 mm, while the lower flexural reinforcement (compression side) was reinforced with 6 mm steel bars spaced at 200 mm with concrete cover 10 mm. The average effective depth and reinforcement ratio were 91 mm and 1.124%, respectively for all tested slabs. The material properties of all shear bolts, reinforcing bars, and concrete are illustrated in Table 1.

Each specimen was subjected to central monotonic static loading until failure, using a hydraulic jack positioned under the slab, utilizing a square steel plate of 200×200 mm² and 50 mm in thickness. The slabs were anchored to the strong laboratory floor at eight points using four steel tendons and spreader beams, as shown in Figure 2. The loading was implemented in two successive steps. The slabs were first subjected to about 60% of the experimental ultimate load of the reference specimen (R), then released, and shear-reinforced throughout the cracking stage.

Table 1. Material properties of all tested slabs [28]

Specimen		R	M8A	M8	M8S	M8SE	M6	M6S	M6SE
Anchorage type			L	L	S	SE	L	S	SE
Bolt type			M8	M8	M8	M8	M6	M6	M6
Bolt initial force on (kN)			1.3	5.9	5.5	6.0	3.5	2.7	2.7
f'_c (MPa)		41.70	50.90	50.66	41.14	28.47	50.66	38.59	28.47
f'_t (MPa)		2.13	2.35	2.35	2.11	1.76	2.35	2.05	1.76
E_c (GPa)		35.51	39.24	39.14	35.27	29.34	39.14	38.59	29.34
M6	$f_y/f_{0.2}$ (MPa)					523	586		523
	f_t (MPa)					618	696		618
M10	$f_y/f_{0.2}$ (MPa)					529	467		529
	f_t (MPa)					653	597		653
M6	$f_{0.2}$ (MPa)						421	530	530
	E_w (GPa)						197	195	195
M8	$f_{0.2}$ (MPa)		523	523	587	587			
	E_w (GPa)		200	200	217	217			

S: small end anchorage; L: large end anchorage; SE: small embedded anchorage

$$f'_t = 0.33\sqrt{f'_c}$$
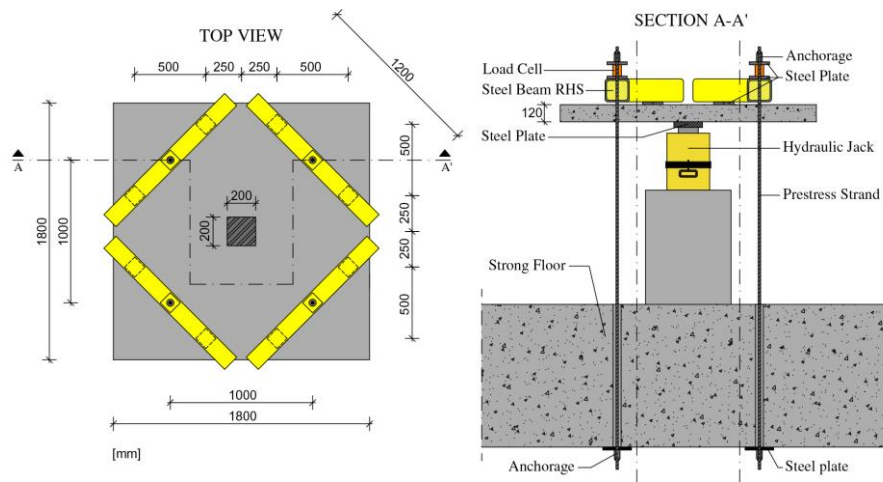$$E_c = 5500\sqrt{f'_c}$$

3676

Figure 2. Support details and test geometry [28]

2.2 Strengthening procedure

The strengthening method is succinctly described as the drilling of 16 small circular holes arranged radially around the loading area (200 mm × 200 mm). The diameters of the drilled holes were 13 mm, 11 mm, and 9 mm for specimens reinforced with shear bolts 10 mm, 8 mm, and 6 mm, respectively. The space between the shear bolts and the drilled holes remained unfilled. Subsequently, the shear bolts were inserted and tightened against the anchorages on slab surfaces. The end anchorages of shear bolts on slab surfaces are divided into three types small embedded anchorage (SE), small anchorage on surface (S), and large anchorage on surface (L), as illustrated in Figure 3. The punching shear reinforcement consisted of sixteen vertical shear bolts placed in radial rows adjacent to the column. The initial row was positioned around 0.5 d (50 mm) from loading zone, while the next layer was situated about 0.75 d (75 mm) from the initial layer. Figure 4 shows the details of the anchoring plates and anchorage zone.
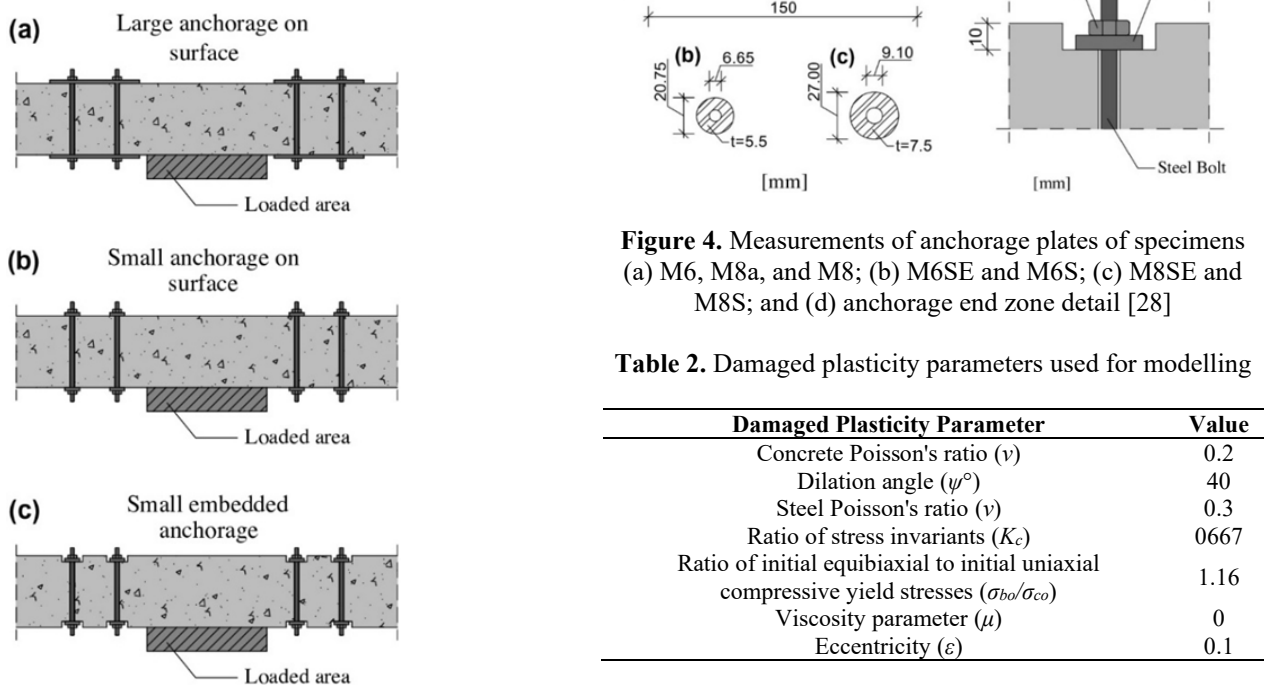

Figure 3. Types of end anchorages of shear bolts on slab surfaces [28]

3. FINITE ELEMENT MODELLING

3.1 Common modelling parameters for all slabs

Three-dimensional non-linear analysis was conducted using the finite element ABAQUS software on slab-column interior junctions strengthened by shear bolts. The CDP model was utilised to study the non-linear behaviour of concrete slabs, encompassing inelastic deformation, crushing, cracking, and the degradation of stiffness. The damaged concrete plasticity model was previously employed in the analysis of slab SB1 without strengthening [29]; the same procedure is used herein for modelling all slabs. The parameters used for the damaged plasticity model are listed in Table 2.

Figure 4. Measurements of anchorage plates of specimens (a) M6, M8a, and M8; (b) M6SE and M6S; (c) M8SE and M8S; and (d) anchorage end zone detail [28]

Table 2. Damaged plasticity parameters used for modelling

Damaged Plasticity Parameter	Value
Concrete Poisson's ratio (v)	0.2
Dilation angle ($\psi°$)	40
Steel Poisson's ratio (v)	0.3
Ratio of stress invariants (K_c)	0667
Ratio of initial equibiaxial to initial uniaxial compressive yield stresses (σ_{bo}/σ_{co})	1.16
Viscosity parameter (μ)	0
Eccentricity (ε)	0.1

The concrete was modelled using 8-node hexahedral brick elements (C3D8R) with reduced integration [30-32]. Both the compression and tension responses of the concrete were modelled with the use of the Hognestad parabola and the

stress-crack displacement relationship, respectively. The tensile behaviour was defined by a bilinear tension-softening response, necessitating key concrete parameters, including the maximum tensile strength f'_t and the fracture energy G_f. The parameter G_f denotes the area beneath the tensile stress-crack displacement curve, which is affected by the size of the aggregate and concrete's quality. The CEB-FIP Model Code 1990 [33] was adopted for estimating G_f as follows:

$$G_f = G_{fo}(f_{cm}/f_{cmo})^{0.7} \qquad (1)$$

The steel material, including reinforcing flexural bars, shear bolts, nuts, washers, and loading plates, were modelled utilizing truss elements (T3D2). They were defined using the uniaxial stress-plastic strain relationship. Their plastic behaviour was outlined using a data table that included yield stress and the corresponding plastic strain. The embedding technique was used to mimic an ideal bond between reinforcing bars and concrete. Compression and tension damage criteria were ignored due to monotonic loading. The tie constraint was used to delineate the interaction between the surfaces of the loading plate and the concrete. This kind of restriction effectively inhibits movement between two sets of surfaces, despite their differing mesh sizes.

Due to all slabs having identical geometry, a quarter of each was considered for analysis. The test slabs were analysed via quasi-static analysis in ABAQUS. This method necessitates applying a low velocity to guarantee precise outcomes. Thereby, all slab models were displaced at 20 mm/s, which gradually increased according to a smooth amplitude curve from 0 mm/s to 40 mm/s. The slab models were restrained against vertical displacement at their perimeters. Figure 5 depicts the typical geometry and boundary conditions for the slab models used in the simulations. The slab vertical deflection Δ was measured at the centre of each slab.
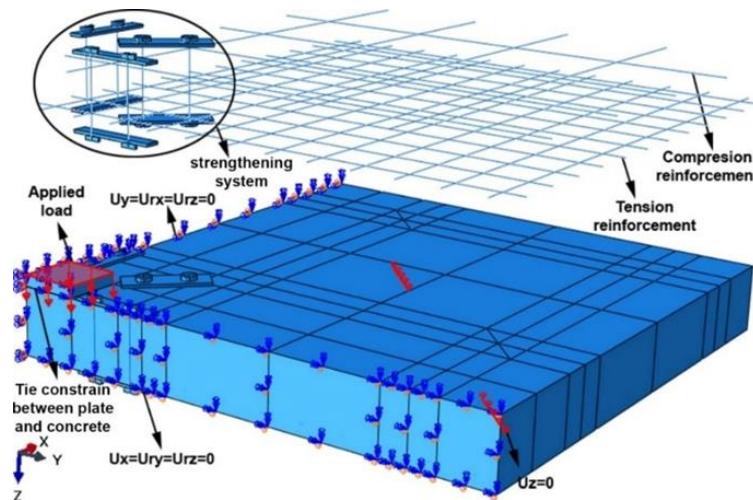

Figure 5. Depicts the typical geometry and boundary conditions for the slab models used in the simulations

A finite element sensitivity analysis was conducted on reference slab model (R) using mesh sizes of 15 mm, 20 mm, and 30 mm. Based on this study, a 20 mm mesh size was selected for the calibration process. This decision was based on the convergence of results and the agreement between finite element and experimental observations particularly in terms of load-deflection responses, cracking patterns and flexural reinforcement behaviour. Figure 6 presents a sensitivity analysis for slab model R for three different mesh sizes (15, 20, and 25).
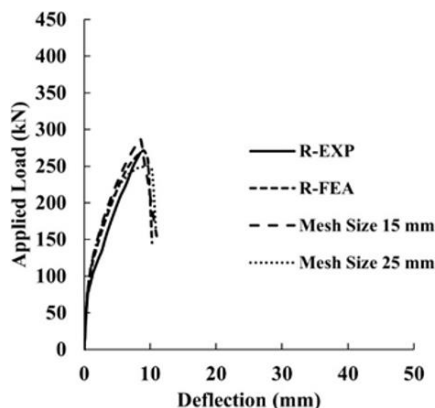

Figure 6. Sensitivity analysis for slab model R

3.2 Modelling of shear bolts

The strengthening strategy against punching shear involves using shear bolts with different end anchorages (small, large, and SEs on slab surfaces). Three types of elements in the ABAQUS material library could be used for modelling shear bolts and their anchorages; these elements involve beam, shell, and solid elements. The truss element type was excluded because it resists only compression and tension forces, contrary to the beam element. To study different kinds of modelling approaches for shear bolts, the test slabs (M8S and M8) were selected to represent the slabs with small and large end anchorages, respectively. The goal is only to identify the best element type for shear bolts and their anchorages that would apply to other slabs. For simplicity, a flowchart was designed to illustrate the modelling techniques used for shear bolts, as shown in Figure 7.

For shear bolts with small anchorages, four different modelling approaches were considered. Solid elements for shear bolts and anchorages (model S1), beam elements for shear bolts without anchorages (model S2), and beam elements for shear bolts with solid anchorages. In the last kind, the joint between the shear bolt and its anchorages was modelled once constrained (model S3) and once unconstrained (model S4). For the constrained type, the coupling constraint type was used (Ux = Uy = Uz = 0). More details are listed in Table 3 and

shown in Figure 8.

For shear bolts with large anchorages, seven modelling methods were presented. Assembled beam elements for both shear bolts and their anchorages (model L1), two types of sloid element systems for shear bolts and their anchorages (models L2 and L3), two types of shell element systems for shear bolts and their anchorages (models L4 and L5), and beam elements for shear bolts and solid elements anchorage (models L6 and L7). In the last kind, the joint between the shear bolts and their anchorages was modelled once constrained and once unconstrained. More details are listed in Table 3 and shown in Figure 9.
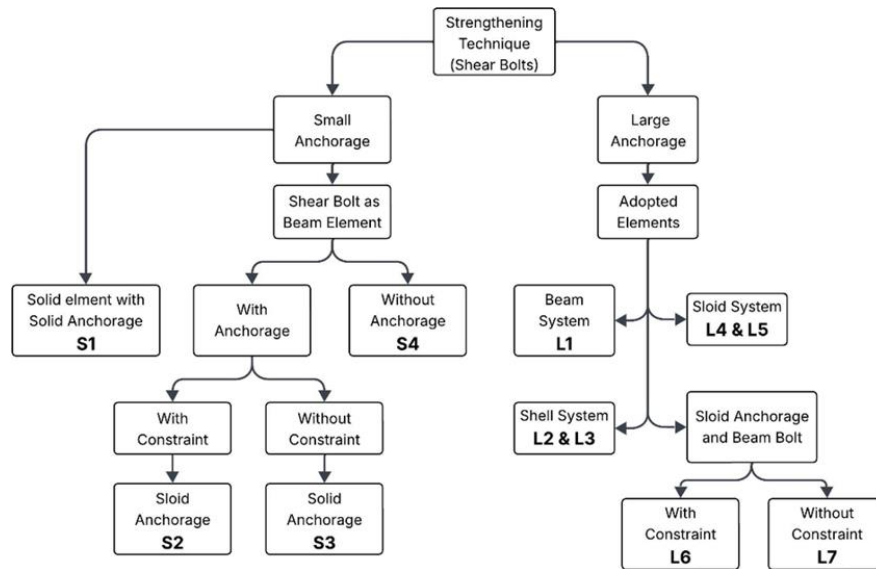

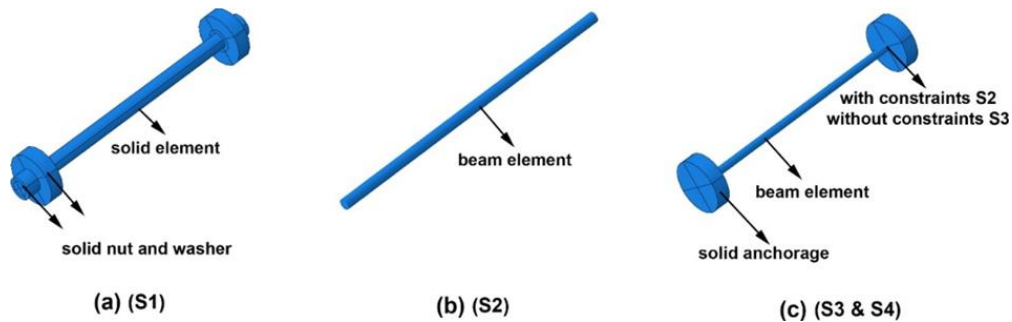**Figure 7.** Flowchart of the used modelling strategies of shear bolts for slab models M8S and M8

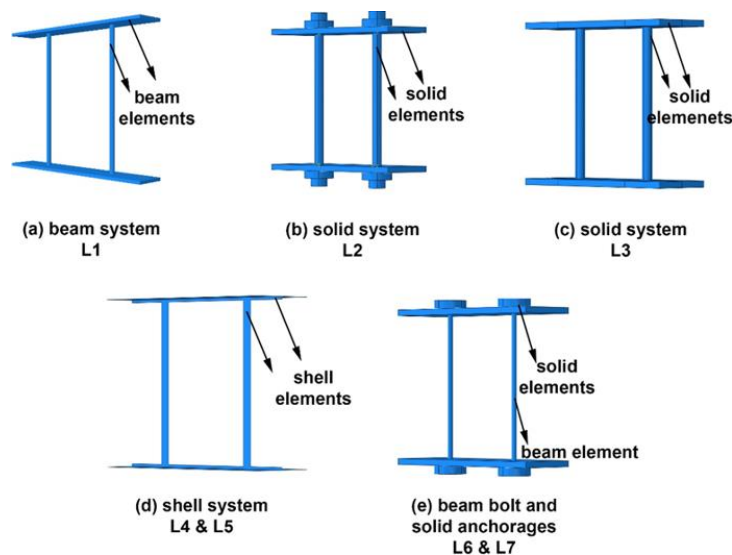**Figure 8.** Modelling techniques for shear bolts with small anchorages for slab model M8S

Figure 9. Modelling techniques for shear bolts with large anchorages for slab model M8

**Table 3.** Details of modelling strategies for shear bolts and their anchorages

Anchorage Type	Modeling Strategy	Adopted Slab	Used Elements		Join Between Shear Bolts and Anchorages	Contact Between Anchorages and Other Surfaces
			Shear Bolts	Anchorages		
Small anchorage	S1	M8S	Solid	Solid	Integrated	Tie constrain
	S2		Beam	-	-	-
	S3		Beam	Solid	Coupling constrain	Tie constrain
	S4		Beam	Solid	-	Tie constrain
Large anchorage	L1	M8	Beam	Beam	Integrated	Embedded method
	L2		Solid	Solid	Integrated	Tie constrain
	L3		Solid	Solid	Integrated	Tie constrain
	L4		Shell	Shell	Integrated	Embedded method
	L5		Shell	Shell	Integrated	Tie constrain
	L6		Beam	Solid	Coupling constrain	Tie constrain
	L7		Beam	Solid		Tie constrain

Table 4. Ultimate failure loads and central deflection for all proposed modelling strategies

|	Slab Model M8S				Slab Model M8						
	$V_{max, exp}$ = 352.3 kN				$V_{max, exp}$ = 381 kN						
Modelling strategy	S1	S2	S3	S4	L1	L2	L3	L4	L5	L6	L7
$V_{max, FEA}$	349	338	344	**349**	392	386	393	401	397	373	**371**
$\Delta_{max, FEA}$	19	19	20	19	19	21	23	21	22	21	21

3.3 Optimal modelling strategy for shear bolts

Eleven modelling strategies for shear bolts and their anchorages, both small and large, were proposed and examined. Figure 10 indicates that all proposed strategies demonstrated satisfactory performance in the load-deflection behaviour relative to the experimental slabs (M8S and M8). Additionally, all strategies generated similar crack patterns on the tension surfaces when compared to the corresponding test slabs (M8S and M8). The ultimate failure loads and their corresponding central deflection for all proposed modelling strategies are illustrated in Table 4.
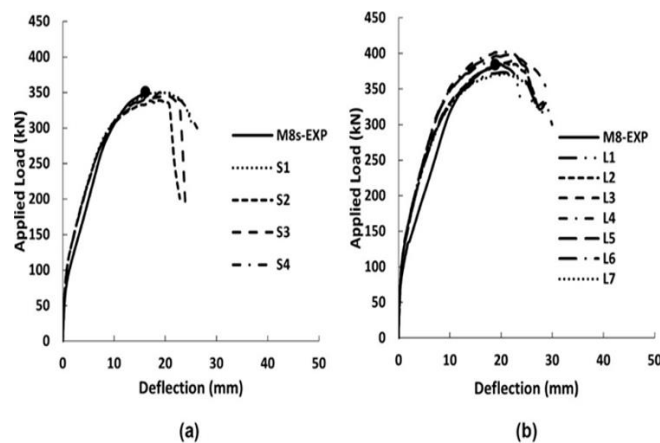
Figure 10. Numerical load-deflection behaviour for slab models (a) M8S and (b) M8 for various shear bolts modelling strategies

For the slab M8S (shear bolts with small anchorages), the modelling strategy S4 (beam elements for shear bolts and solid elements for anchorages) showed optimal performance in terms of load-deflection response, crack pattern on the tension surface, straightforward modelling, and less computational time. The other modelling strategies (S1, S2, and S3) demonstrated acceptable results regarding the previously mentioned criteria. However, while modelling strategies S1

and S3 showed acceptable results, they required more time for both modelling and computation. Furthermore, the modelling strategy S2, which uses shear bolts without anchorages, showed results that were below the required level when compared to the other modelling strategies.
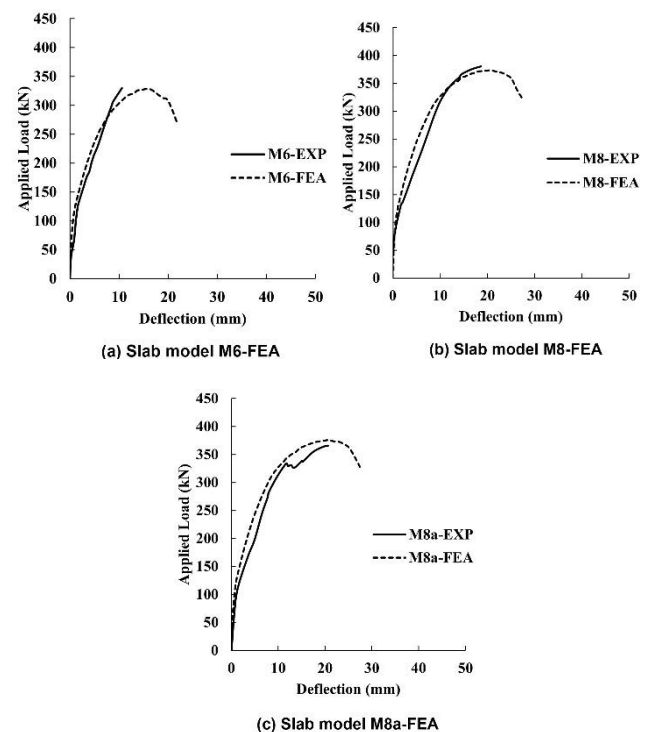
Figure 11. Load-deflection curves for strengthened slabs with large anchorages using modelling strategy L7

Regarding the slab M8 (shear bolts with large anchorages), the model strategy L7 (beam elements for shear bolts and solid elements for anchorages) revealed superior performance in terms of load-deflection response, crack pattern on the tension surface, straightforward modelling, and computational time. Other modelling strategies (L1 to L6) exhibited satisfactory outcomes concerning the aforementioned criteria.

Nevertheless, whereas these modelling strategies achieved satisfactory outcomes, they necessitated more time for both modelling and computation.
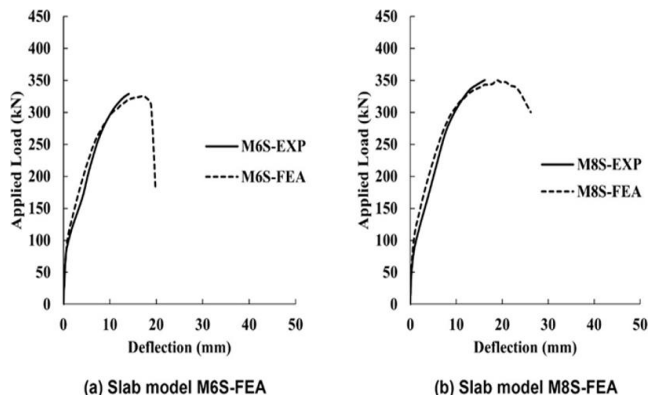

(a) Slab model M6S-FEA

(b) Slab model M8S-FEA

Figure 12. Load-deflection curves for all strengthened slabs with small anchorages using modelling strategy S4

(b) Slab model M6SE-FEA
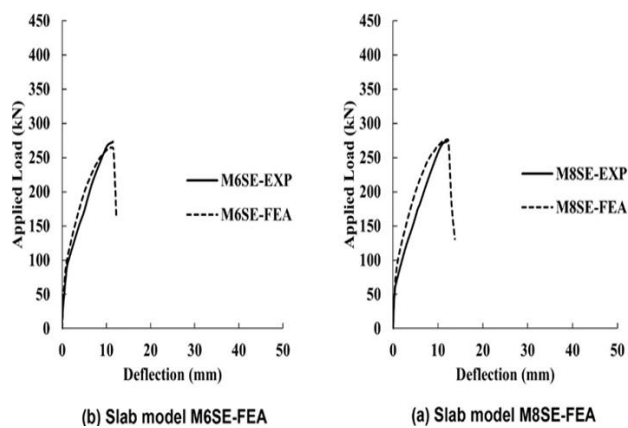
(a) Slab model M8SE-FEA

Figure 13. Load-deflection curves for strengthened slabs with SEs using modelling strategy S4

(a) Slab model R

(b) Slab model M6S

(c) Slab model M8S

(d) Slab model M6

(e) Slab model M8

(f) Slab model M8a

(g) Slab model M6SE
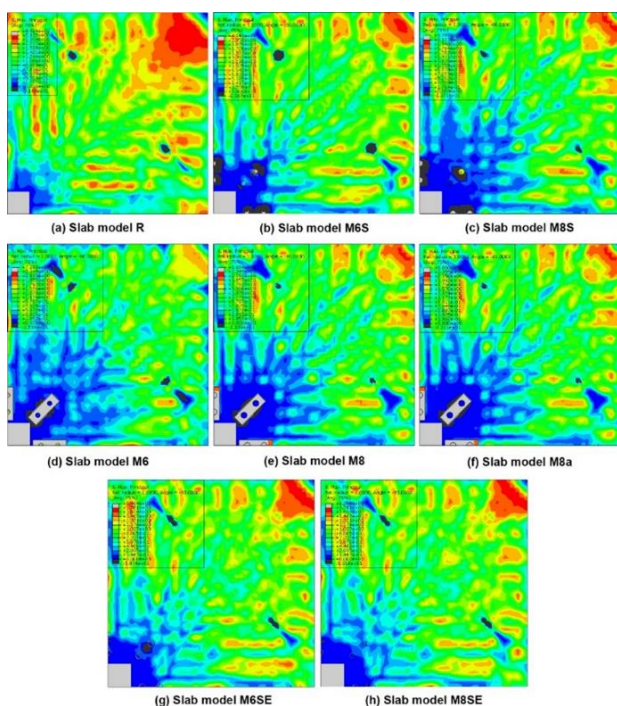
(h) Slab model M8SE

Figure 14. Crack patterns on tension surface for all slab models

Notes: Cracked regions are presented via the blue contours

The modelling strategies S4 and L7 are most effective for modelling shear bolts and their anchorages in slabs strengthened with shear bolts featuring small and large end anchorages, respectively. Consequently, these two modelling strategies are implemented on the remaining strengthened slabs. Figures 11-13 present a comparison of the load-deflection curves of all strengthened slabs for large, small, and SEs, respectively. Figures 14 and 15 depict the crack patterns observed on the tension surfaces of all slab models and the test slabs (M6, M6S, and M6SE). Obvious cracks formed within the enhanced zone for slab models M6, M8a, M6S, M6SE, and M8SE. Consistent with the test findings, these slab models failed in punching mode within enhanced zone [17]. The other slab models failed in the flexural mode linked to punching failure outside the enhanced zone. The consistency between the finite element analysis and the experimental findings regarding load-deflection responses and crack patterns refers to the verified models' ability to evaluate additional parameters.
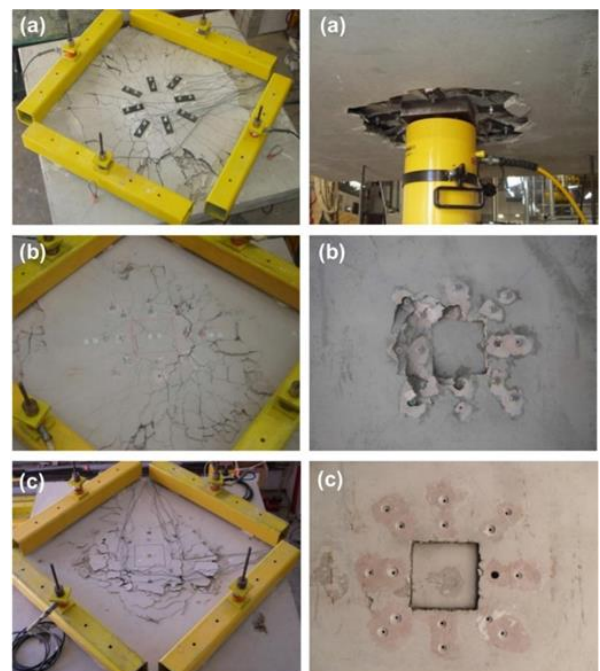

Figure 15. Top view (left) and bottom view (right) of specimens (a) M6, (b) M8S and (c) M6SE [28]

4. PROMETRIC STUDIES

Parametric analyses were conducted to examine various essential parameters concerning the thickness of end anchorages and the potential configurations of shear reinforcements. Three groups of shear-reinforced slabs were established in this context. Group I consists of shear-reinforced slabs with various thicknesses of large anchorages: 8 mm, 10 mm, and 12 mm for slab models M8-8 mm, M8-10 mm, and M8-12 mm, respectively. Group II consists of shear-reinforced slabs featuring different arrangements of shear bolts with large anchorages. Group III comprises shear-reinforced slabs with various arrangements of shear bolts with small anchorages. Figure 16 illustrates the arrangement of shear bolts for all parametric slab models in established groups I, II and III and the critical control perimeter based on ACI 318 and Eurocode 2. Slab M8 was selected to represent the

strengthened slab in groups I and II, while slab M8S was designated to represent the strengthened slab in group III in terms of geometry and material properties.
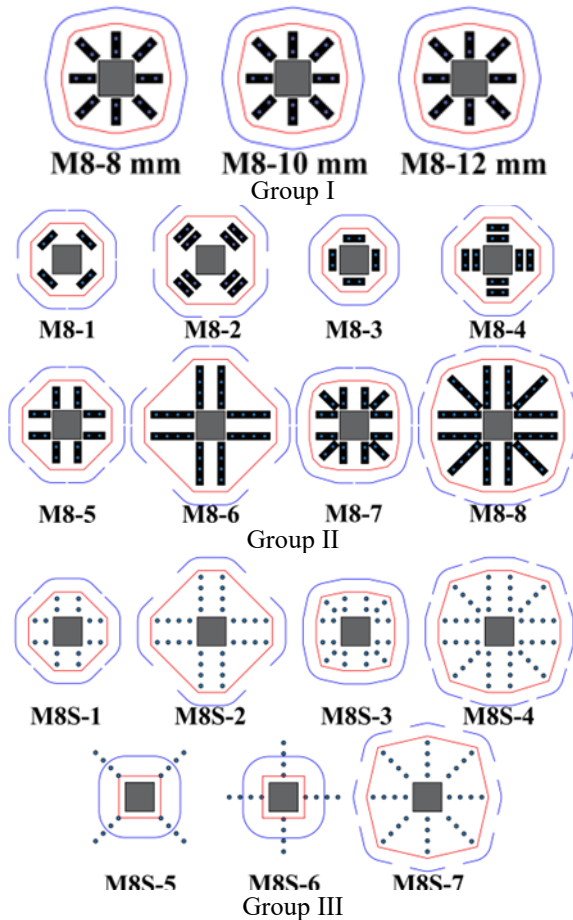

Figure 16. Parametric slab models of Groups I, II and III and their punching shear control perimeter based on design codes
Notes: —(in red) Control Perimeter according to ACI 318; —(in blue) Control Perimeter according to Eurocode 2

5. FINITE ELEMENT RESULTS

The slab models (M8-8 mm, M8-10 mm, and M8-12 mm) in Group I demonstrated similar behaviour in terms of load-deflection and failure mode. This suggests that augmenting the anchoring thickness has not affected the punching shear strength. The reason is that the increasing the anchoring thickness kept the critical section unchanged. Nonetheless, increasing the anchoring thickness somewhat improved the punching capacity by about 3% relative to slab model M8-FEA, as seen in Figure 17(a). Increasing the anchorage thickness resulting in increasing the confining pressure between them. Thus, these slab models exhibited a marginal, almost imperceptible enhancement in initial stiffness, ductility, and energy absorption relative to slab model M8-FEA. Moreover, all these slab models recorded ultimate strength higher than the specified flexural strength of the unenhanced slab (V_{flex} = 328 kN). Hence, all these slabs were failed in flexural mode, which is finally associated with punching failure outside the shear-enhanced region. The crack pattern on the tension surface was similar to that crack pattern formed in slab model M8-FEA, as shown in Figure 14(e).

The slab models M8-2, M8-6, M8-7, and M8-8 in Group II exhibited satisfactory outcomes concerning punching capacity

and failure mode. The enhancement in punching capacity for these slab models was approximately 3%, 4%, 5%, and 18%, respectively, compared to the slab model M8-FEA, as depicted in Figure 17(b). This is attributed to the supporting zone being well expanded when adopting such arrangements. Additionally, if compared to the other slab models in the same group, the slab model M8-8 recorded an increase in energy absorption and ductility of about 164% and 25%, respectively, over the slab model M8-FEA. This is attributed to the increased confining pressure resulting from the presence of radial placement of shear bolts. Besides, all the slab models in this group exhibited well-defined crack patterns on the tension surfaces, as shown in Figure 18. However, the punching capacity of the other slab models (M8-1, M8-3, M8-4, M8-5, and M8-7) in this group was inferior to that of the slab model M8-FEA. Moreover, all of the slab models in this group recorded a flexural failure mode associated with punching shear outside the shear-enhanced zone except for slab model M8-3, which failed in punching mode beyond the shear-reinforced zone. This failure occurred due to the placement of the shear bolt within a distance equivalent to d = 50 mm (within the critical section). Additionally, the ultimate strength recorded by all slab models exceeded the flexural strength of the unenhanced slab (V_{flex} = 328 kN), except for slab model M8-3. Moreover, the slab model M8-6 exhibited a better post-failure response compared to other slab models. This phenomenon is attributed to the slight confining pressure applied between anchorages, resulting from the absence of the radial placement of shear bolts.
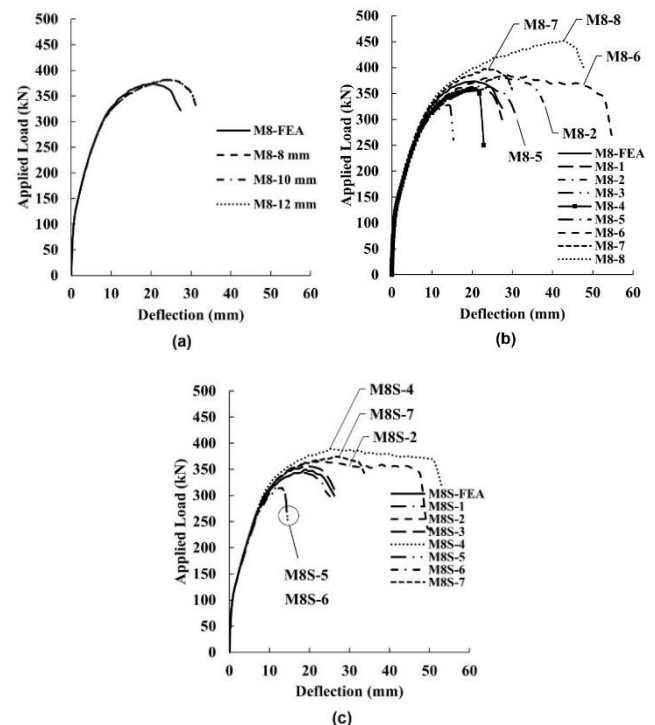

Figure 17. Load-deflection behaviour of parametric slab models in a) Group I, b) Group II, and c) Group III

The slab models M8S-2, M8S-4 and M8S-7 in Group III demonstrated satisfactory outcomes regarding punching capacity and crack patterns on the tension surfaces. The enhancement in punching capacity for these slab models was on average 7% compared to the slab model M8S-FEA, as depicted in Figure 17(c). These configurations embrace and beyond the critical section around the supporting region,

signifying their effectiveness. The other slab models in this group recorded punching strength equal to slab model M8S-FEA, except slab models M8S-5 and M8S-6, which recorded punching strength lower to slab model M8S-FEA. Only the slab model M8S-4 failed in flexural mode, which is finally associated with punching shear outside the shear-reinforced region. Except for slab models M8S-5 and M8S-6, which failed in punching shear within the shear-reinforced zone.

Indicating to insufficient amount of shear reinforcement around the supporting zone. The others failed in punching shear mode outside the shear-reinforced zone before attaining the ultimate flexural strength ($V_{flex} = 378$ kN). The evidence suggests that these arrangements are unfavourable. Figure 18 displays the crack patterns on the tension surface for all slab models in this group.
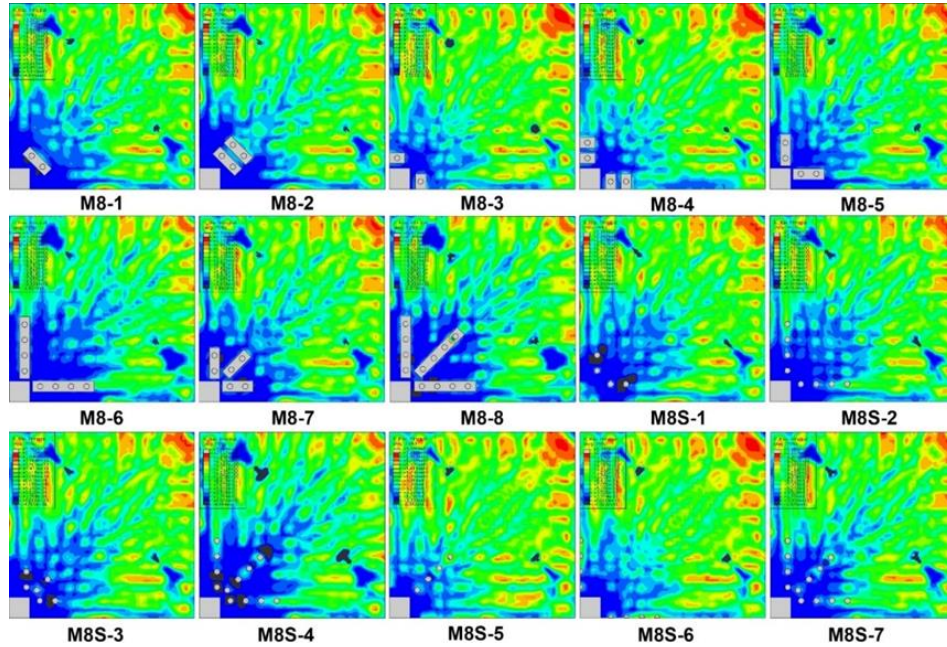

Figure 18. Crack patterns on tension surfaces of parametric slab models

The radial arrangement of shear reinforcement had substantial outcomes, especially for the ultimate strength and failure mode, in contrast to other arrangements. The radial arrangement of shear reinforcement provided a better enhancement to the flexural reinforcement, extended the critical section surrounding the support region, and alleviated stress concentration at column corners, particularly in case of adopting shear bolts with large end anchorages.

Shear bolts with large anchorages demonstrated superior mobilisation for flexural reinforcement compared to shear bolts with small anchorages. The large anchorages not only enhanced the flexural reinforcement but also amplified the critical section around the column. Furthermore, the flexural reinforcement commenced activation at a deflection of 2.4 mm across all reinforced slab models.

Small stresses were detected in the shear bolts until the maximum load of the slabs was attained. Only the first bolt commenced activation at a deflection of 10 mm. Typically, the bolts of all slabs began to engage at loads above the ultimate load of the specimen devoid of shear reinforcement (R), since cracking occurred at comparable load levels for all slabs with and without shear reinforcement. The first row of bolts endures more stresses than the following rows because of the shear cracks located near the column.

6. CODES EVALUATION

Flat slabs generally experience failure due to flexural or punching shear. Punching shear strength is calculated by delineating the critical section (control perimeter) around the

column. This perimeter is positioned at 0.5 d and 2 d (where d = effective depth of the slab), respectively, from the column face in unstrengthened slabs, as per ACI318 [34] and Eurocode 2 [35]. Additionally, both codes necessitate the evaluation of punching shear outside the shear-enhanced region, with control perimeters established at 0.5 d and 1.5 d from the shear-reinforced zone for ACI 318 and Eurocode 2, respectively. The parametric slab models exhibited two major failure modes: either punching shear outside the enhanced zone or flexural failure associated with punching shear failure beyond the shear-reinforced zone. The only exception to this rule was the slab models M8S-5 and M8S-6, which failed due to punching shear inside the enhanced zone. So, the used equations for calculating punching shear strength inside and outside the shear-reinforced zone based on design code ACI 318-25 are given in Eqs. (2) and (3), respectively.

$$V_{n,ACI} = \overbrace{0.75 * 0.33\lambda_s\lambda\sqrt{f'_c}b_o d}^{V_{c,ACI}} + \overbrace{(A_v f_{yt} d/S)}^{V_S} \qquad (2)$$

$$V_{out,ACI} = 0.17\lambda\lambda_s b_{out} d\sqrt{f'_c} \qquad (3)$$

where, $V_{n,ACI}$: nominal shear strength of slab within the shear-reinforced zone; $V_{c,ACI}$: shear strength provide by concrete; V_s: shear strength provide by shear bolts, A_v: area of shear bolts within the control perimeter; f_{yt}: yield strength of shear bolts (≤ 420 MPa); s: spacing between shear bolts; λ: modification factor of lightweight concrete (for normal weight concrete, $\lambda = 1$); λ_s: size effect modification factor equals $(2/(1 + 0.004 d)^{0.5} \leq 1)$; b_o: control perimeter inside the enhanced zone; f'_c:

compressive strength of concrete-based cylinder test; d: effective depth of the slab; $V_{out, ACI}$: punching shear strength

outside shear-reinforced zone; b_{out}: control perimeter outside the enhanced zone.

Table 5. Punching shear predictions according to design codes ACI 318 and Eurocode 2

Group	Slab Model	ACI 318-19		Eurocode 2		V_{FEA} (kN)	$V_{ACI}/$ V_{FEA}	$V_{EC2}/$ V_{FEA}	Failure Mode
		b_{out} (mm)	V_{ACI} (kN)	b_{out} (mm)	V_{EC2} (mm)				
Group I	M8-8 mm	2071	228	2693	339	381	0.60	0.89	Flexural/punching outside
	M8-10 mm	2071	228	2693	339	381	0.60	0.89	Flexural/punching outside
	M8-12 mm	2071	228	2693	339	381	0.60	0.89	Flexural/punching outside
Group II	M8-1	1702	187	2185.68	275	358	0.52	0.77	Flexural/punching outside
	M8-2	2126	234	2185.68	275	382	0.61	0.72	Flexural/punching outside
	M8-3	1467	162	2028.08	256	327	0.49	0.78	Punching outside
	M8-4	1892	208	2188.4	276	357	0.58	0.77	Flexural/punching outside
	M8-5	2035	224	2313.68	292	364	0.62	0.80	Flexural/punching outside
	M8-6	2883	317	2313.68	292	385	0.82	0.76	Flexural/punching outside
	M8-7	2185	241	2646.72	334	397	0.61	0.84	Flexural/punching outside
	M8-8	3104	342	3056.44	385	448	0.76	0.86	Flexural/punching outside
Group III	M8S-1	1764	175	2185.68	257	343	0.51	0.75	Punching outside
	M8S-2	2613	259	2185.68	257	367	0.71	0.70	Punching outside
	M8S-3	1942	193	2482.84	292	358	0.54	0.81	Punching outside
	M8S-4	2841	282	2912.72	342	389	0.72	0.88	Flexural/punching outside
	M8S-5	1164	327 [Eq (2)]	1,943.52	343 [Eq (4)]	317	1.03	1.08	Punching inside
	M8S-6	1164	327 [Eq (2)]	1,943.52	343 [Eq (4)]	313	1.04	1.09	Punching inside
	M8S-7	2830	281	2312.92	272	374	0.75	0.73	Flexural/punching outside
Average							0.673	0.834	
Standard of deviation							0.160	0.111	

Likewise, the used equations for calculating punching shear strength inside and outside the shear-reinforced zone based on design code Eurocode 2 are given in Eqs. (4) and (5), respectively.

$$V_{n,EC2} = \overbrace{\left(0.18k(100\rho f_{ck})^{1/3}b_o d \geq V_{min} = 0.035(k)^{3/2}\sqrt{f_{ck}}b_o d\right)}^{V_{c,EC2}} + \overbrace{\left(1.5A_{se}f_{yte}d/S\right)}^{V_{se}} \quad (4)$$

$$V_{out,Ec2} = 0.18kb_{out}d(100\rho f_{ck})^{1/3} \geq V_{min} = 0.035(^k\sqrt{f_{ck}}b_{out}d) \quad (5)$$

where, k: size effect factor ($k = 1 + \sqrt{200/d} \leq 2$); ρ: flexural reinforcement ratio; f_{ck}: characteristic compressive strength of concrete; $V_{n, ACI}$: nominal strength of slab within the shear-reinforced zone; A_{se}: area of shear bolts within the control perimeter; V_{se}: shear strength provided by shear bolts; f_{yte}: effective design strength of the shear bolts ($f_{yte} = 1.15 (250 + 0.25\ d) \leq f_{yt}$). Table 5 compares punching shear predictions based on the design codes considered.

7. CONCLUSIONS

Finite-element simulations of shear-reinforced concrete flat slabs using shear bolts were conducted using the CDP model to investigate ultimate load, cracking propagation, and central deflection of shear-reinforced interior slab-column junctions. Accurate numerical predictions require proper modelling process, and the calibrated CDP model adopted from Slab SB1 without shear bolts has been shown to reliably capture the structural responses of shear-reinforced slabs. In this study, shear bolts and their end anchorages were represented as beams and solid elements, respectively, and various modelling strategies were explored to simulate their behaviours. Eight flat slabs from previous experimental work were numerically examined in ABAQUS, considering different shear bolt arrangements and end anchorages (small and large). Furthermore, the study evaluated the impact of various arrangements of shear bolts and the thickness of their anchorages on punching resistance by conducting a parametric analysis. This study draws conclusions only from numerical findings, as follows:

1. The numerical calibration results pointed out that the optimal modelling strategy was to use beam elements for shear bolts and solid elements for their anchorages, regardless of whether the anchorages are small or large, and an unconstrained (coupling constraint is overlooked) joint between shear bolts and their anchorages. This method established a dependable baseline for simulation; however, its applicability remains confined to the static loading conditions.

2. The other modelling strategies for shear bolts and their anchorages have shown acceptable representations in terms of load-deflection responses and crack patterns. But these modelling strategies are complex and require a lot of efforts and computational time. Furthermore, using shear bolts solely without anchorages demonstrated unacceptable behaviour compared to other modelling strategies.

3. The majority of the strengthened slab models exhibited a flexural failure mode associated with punching shear beyond the shear-reinforced zone. The probability of such a failure mode escalates with the increasing quantity of dispersed shear bolts around the column. However, the radial arrangement of shear bolts with large anchorages demonstrated enhanced performance for load-deflection responses and deformation capacity.

4. Certain slab models either experienced failure due to punching shear outside the shear-reinforced zone (slab model M8-3) or failed in punching shear inside the shear-reinforced zone (slab models M8S-5 and M8S-6). This suggests that the shear reinforcement was not properly arranged. This highlights a critical area for future refinement in design guidelines.

5. Shear bolts with larger anchorages enhanced the mobilization of flexural reinforcements. The effect is evident

in the crack propagation towards the slab edges and corners. This highlights the importance of designing the shear bolts' anchorages for better structural performance.

6. Both the design codes demonstrated conservative predictions; ACI 318 was more conservative than Eurocode 2. However, both of them overestimated punching shear resistance for the slab models M8S-5 and M8S-6. Indicating that these design codes may.

7. Future research needs to expand this analysis to include dynamic loading conditions for assessing performance during seismic or impact events, and to explore a broader spectrum of geometric and material parameters to provide more generalised design recommendations.

ACKNOWLEDGMENT

REFERENCES

[1] Dilger, W.H., Ghali, A. (1981). Shear reinforcement for concrete slabs. Journal of the Structural Division, 107(12): 2403-2420. https://doi.org/10.1061/JSDEAG.0005846

[2] Broms, C.E. (2007). Ductility of flat plates: Comparison of shear reinforcement systems. ACI Structural Journal, 104(6): 703-711. https://doi.org/10.14359/18952

[3] Robertson, I.N., Kawai, T., Lee, J., Enomoto, B. (2002). Cyclic testing of slab-column connections with shear reinforcement. ACI Structural Journal, 99(5): 605-613. https://doi.org/10.14359/12300

[4] Caldentey, A.P., Lavaselli, P.P., Peiretti, H.C., Fernandez, F.A. (2013). Influence of stirrup detailing on punching shear strength of flat slabs. Engineering Structures, 49: 855-865. https://doi.org/10.1016/j.engstruct.2012.12.029

[5] Broms, C.E. (2019). Cages of inclined stirrups as shear reinforcement for ductility of flat slabs. ACI Structural Journal, 116(1): 77-88. https://doi.org/10.14359/51711276

[6] Almeida, A.F., Alcobia, B., Ornelas, M., Marreiros, R., Ramos, A.P. (2020). Behaviour of reinforced-concrete flat slabs with stirrups under reversed horizontal cyclic loading. Magazine of Concrete Research, 72(7): 339-356. https://doi.org/10.1680/jmacr.18.00347

[7] Raafat, A., Fawzi, A., Metawei, H., Abdalla, H. (2021). Assessment of stirrups in resisting punching shear in reinforced concrete flat slab. HBRC Journal, 17(1): 61-76. https://doi.org/10.1080/16874048.2021.1881422

[8] Corley, W.G., Hawkins, N.M. (1968). Shearhead reinforcement for slabs. Journal Proceedings, 65(10): 811-824. https://doi.org/10.14359/7514

[9] Bompa, D.V., Elghazouli, A.Y. (2016). Structural performance of RC flat slabs connected to steel columns with shear heads. Engineering Structures, 117: 161-183. https://doi.org/10.1016/j.engstruct.2016.03.006

[10] Bompa, D.V., Elghazouli, A.Y. (2020). Nonlinear numerical simulation of punching shear behavior of reinforced concrete flat slabs with shear-heads. Frontiers of Structural and Civil Engineering, 14(2): 331-356. https://doi.org/10.1007/s11709-019-0562-y

[11] Tan, Y., Teng, S. (2005). Interior slab-rectangular column connections under biaxial lateral loadings. Special Publication, 232: 147-174. https://doi.org/10.14359/14941

[12] Dam, T.X., Wight, J.K. (2016). Flexurally-triggered punching shear failure of reinforced concrete slab-column connections reinforced with headed shear studs arranged in orthogonal and radial layouts. Engineering Structures, 110: 258-268. https://doi.org/10.1016/j.engstruct.2016.01.006

[13] Eom, T.S., Song, J.W., Song, J.K., Kang, G.S., Yoon, J.K., Kang, S.M. (2017). Punching-shear behavior of slabs with bar truss shear reinforcement on rectangular columns. Engineering Structures, 134: 390-399. https://doi.org/10.1016/j.engstruct.2016.12.048

[14] Ebead, U., Marzouk, H. (2002). Strengthening of two-way slabs using steel plates. ACI Structural Journal, 99(1): 23-31. https://doi.org/10.14359/11032

[15] Elbakry, H.M., Allam, S.M. (2015). Punching strengthening of two-way slabs using external steel plates. Alexandria Engineering Journal, 54(4): 1207-1218. https://doi.org/10.1016/j.aej.2015.09.005

[16] Bayrak, O., Jirsa, J.O., Tian, Y. (2010). Seismic rehabilitation of slab-column connections. ACI Structural Journal, 107(2): 237. https://doi.org/10.14359/51663540

[17] Fernández Ruiz, M., Muttoni, A., Kunz, J. (2010). Strengthening of flat slabs against punching shear using post-installed shear reinforcement. ACI Structural Journal, 107(4): 434-42. https://doi.org/10.14359/51663816

[18] Wörle, P. (2014). Enhanced shear punching capacity by the use of post installed concrete screws. Engineering Structures, 60: 41-51. https://doi.org/10.1016/j.engstruct.2013.12.015

[19] Adetifa, B., Polak, M.A. (2005). Retrofit of slab column interior connections using shear bolts. ACI Structural Journal, 102(2): 268. https://doi.org/10.14359/14278

[20] Baig, Z.I., Alsayed, S.H., Abbas, H. (2016). Punching of slab-column connections strengthened using external steel shear bolts. Magazine of Concrete Research, 68(2): 55-68. https://doi.org/10.1680/macr.14.00434

[21] Sharaf, M.H., Soudki, K.A., Van Dusen, M. (2006). CFRP strengthening for punching shear of interior slab-column connections. Journal of Composites for Construction, 10(5): 410-418. https://doi.org/10.1061/(ASCE)1090-0268(2006)10:5(410)

[22] Abdullah, A., Bailey, C.G., Wu, Z.J. (2013). Tests investigating the punching shear of a column-slab connection strengthened with non-prestressed or prestressed FRP plates. Construction and Building Materials, 48: 1134-1144. https://doi.org/10.1016/j.conbuildmat.2013.07.012

[23] Koppitz, R., Kenel, A., Keller, T. (2014). Punching shear strengthening of flat slabs using prestressed carbon fiber-reinforced polymer straps. Engineering Structures, 76: 283-294. https://doi.org/10.1016/j.engstruct.2014.07.017

[24] Durucan, C., Anil, Ö. (2015). Effect of opening size and location on the punching shear behavior of interior slab-column connections strengthened with CFRP strips.

Engineering Structures, 105: 22-36. https://doi.org/10.1016/j.engstruct.2015.09.033

[25] El-Salakawy, E.F., Polak, M.A., Soudki, K.A. (2003). New shear strengthening technique for concrete slab-column connections. Structural Journal, 100(3): 297-304. https://doi.org/10.14359/12604

[26] Genikomsou, A.S., Polak, M.A. (2016). Finite-element analysis of reinforced concrete slabs with punching shear reinforcement. Journal of Structural Engineering, 142(12): 04016129. https://doi.org/10.1061/(ASCE)ST.1943-541X.0001603

[27] Genikomsou, A., Polak, M.A. (2017). Finite element simulation of concrete slabs with various placement and amount of shear bolts. Procedia Engineering, 193: 313-320. https://doi.org/10.1016/j.proeng.2017.06.219

[28] Inácio, M.M., Ramos, A.P., Faria, D.M. (2012). Strengthening of flat slabs with transverse reinforcement by introduction of steel bolts using different anchorage approaches. Engineering Structures, 44: 63-77. https://doi.org/10.1016/j.engstruct.2012.05.043

[29] Taresh, H.R., Yatim, M.Y.M., Azmi, M.R. (2021). Punching shear behaviour of interior slab-column connections strengthened by steel angle plates. Engineering Structures, 238: 112246. https://doi.org/10.1016/j.engstruct.2021.112246

[30] Taresh, H.R., Hussein, T.H.A.A., Radzi, A., Md Yatim, M.Y. (2025). Numerical modeling of perforated flat slabs strengthened with angle plates. Structural Concrete. https://doi.org/10.1002/suco.70150

[31] Taresh, H.R., Md Yatim, M.Y., Azmi, M.R. (2021). Finite element analysis of interior slab-column connections strengthened by steel angle plates. Structural Concrete, 22(2): 676-690. https://doi.org/10.1002/suco.201900561

[32] Ali, Y.A., Assi, L.N., Abas, H., Taresh, H.R., Dang, C.N., Ghahari, S. (2022). Numerical investigation on effect of opening ratio on structural performance of reinforced concrete deep beam reinforced with CFRP enhancements. Infrastructures, 8(1): 2. https://doi.org/10.3390/infrastructures8010002

[33] FIB – International Federation for Structural Concrete. (1993). CEB-FIP Model Code 1990: Design Code. Thomas Telford Ltd., London.

[34] American Concrete Institute. (2019). ACI 318-19: Building Code Requirements for Structural Concrete. https://www.concrete.org/Portals/0/Files/PDF/Previews/318-19_preview.pdf.

[35] The European Union. (2004). Eurocode 2: Design of concrete structures—Part 1-1: General rules and rules for buildings. https://www.phd.eng.br/wp-content/uploads/2015/12/en.1992.1.1.2004.pdf.